SCANNING ELECTRON MICROSCOPY WITH POLARIZATION ANALYSIS STUDIES OF Ni–Fe MAGNETIC MEMORY ELEMENTS

J. Unguris, M. R. Scheinfein, R. J. Celotta and D.T. Pierce

National Institute of Standards and Technology

Gaithersburg, MD 20899

Abstract — This paper describes the use of Scanning Electron Microscopy with Polarization Analysis to quantitatively image the magnetic structure of permalloy magnetic memory elements. Various methods of determining the absolute magnitude and direction of the magnetization vector are described. The magnetic domain structures are observed as a function of ion milling time. During ion milling the surface composition is monitored by Auger analysis.

INTRODUCTION

By measuring the spin polarization of secondary electrons generated in a scanning electron microscope, Scanning Electron Microscopy with Polarization Analysis (SEMPA) can directly measure the magnitude and the direction of the magnetization with sub-micron spatial resolution.[1,2] The high spatial resolution capability of SEMPA has been demonstrated for several systems. Quantitative measurements of the total magnetization magnitude and angle, however, have only been successful in systems where the magnetization was already well understood. The problem is that polarization analyzers measure the three separate components of the magnetization vector rather than the vector itself. Therefore, while relative measurements of a single magnetization component are usually sufficient to image the magnetic domains, the determination of the total magnetization vector requires measurements of each magnetization component with all of the non-magnetic, instrumental and sample-related contributions to the polarization removed.

The source for most of these instrumental polarization contributions is the sensitivity of the polarization analyzer to the trajectory of the secondary electrons that are being analyzed. The spin sensitivity of all of the different SEMPA polarization analyzers currently in use is based upon the spin-orbit dependent asymmetric scattering of spin polarized electrons from a high Z material.[3] Determining one polarization component involves measuring a scattering asymmetry, A, given by

$$A = (I_L - I_R)/(I_L + I_R), \qquad (1)$$

where I_L and I_R are the intensity of electrons backscattered to the left and right, respectively. The polarization component is perpendicular to the scattering plane. Note that the asymmetry is insensitive to changes in the intensity. Fluctuations in the incident electron beam intensity, or surface topography that cause secondary electron intensity changes without significant trajectory changes do not affect the polarization. In a detector without instrumental offsets the polarization, P, is simply given by

$$P = A/S \qquad (2)$$

where S is the Sherman function or resolving power of the detector. S is equal to one for a 100% efficient detector and is about 0.1 in practice. In addition to the true asymmetry, additional instrumental asymmetries may also be present. These asymmetries are either the result of intrinsic biases built into the detector, such as differences in the collection efficiency between the left and right channel detectors, or extrinsic affects, such as changes in secondary electron trajectories due to surface topography or scanning of the incident electron beam. Intrinsic apparatus

asymmetries, as well as the detector Sherman function, can be determined by calibrating the detector once using an electron source of known polarization. On the other hand, extrinsic asymmetries are sample dependent and therefore must be accounted for in each measurement.

The problem of extrinsic apparatus asymmetry can be addressed in several different ways: First, the electron optical design of the polarization detector is done in such a way as to minimize the detector's sensitivity to changes in secondary electron trajectories.[4] Second, if all three polarization projections are imaged for a region with multiple domains, then requiring that the magnitude of the magnetization be constant over the entire image may be sufficient to determine the apparatus asymmetries. Finally, for every polarization image a reference image, in which the spin-dependent scattering has been turned off, can also be recorded and the two subtracted to remove spurious asymmetries. We accomplish the latter by using two scattering targets in our polarization analyzer; a gold film target which is spin sensitive and a low-Z graphite target which has all the same instrumental asymmetries as the gold but is without the spin dependent contrast.

We have used all three of these methods in imaging the magnetic structure of thin permalloy magnetic memory elements. These elements have a chevron shape which can support two possible domain structures; one with a single domain wall down the middle of the bit and one with domain walls that form a Y pattern connecting the tips of the chevron. The bistable nature of the domain pattern makes the element a possible candidate for information storage.[5,6] In addition, we were interested in these elements because their relatively low polarization, large topographic contrast, and magnetic fine structure make them challenging samples for full vector imaging using SEMPA.

EXPERIMENTAL

A schematic of the SEMPA apparatus is shown in Figure 1. The apparatus consists of an ultra-high vacuum Auger microprobe and scanning electron microscope to which two orthogonal polarization analyzers were added. The analyzers have been described in detail elsewhere.[7] Briefly, the analyzers work by first accelerating the secondary electrons to 1500 eV and transporting them through electron optics which prepare them for scattering from a gold film. Deflection plates within the electron optics are coupled to the scan of the electron microscope so that any motion of the secondary electron source point due to scanning of the incident beam is cancelled out and the secondary electron beam is stationary at the gold target. The input optics also contain a 90 degree electrostatic deflector which switches the beam from an analyzer that simultaneously measures the two in-plane magnetization components, to an orthogonal one that measures the magnetization component perpendicular to the sample surface along with a redundant in-plane component. Within the detectors the electron beam is decelerated to 150 eV and is scattered from either an evaporated gold film or a graphite target. The scattering asymmetries are recorded and stored in a computer as the incident electron beam is digitally scanned across the sample.

In addition to polarization analyzers the microscope has a cylindrical mirror electron energy analyzer (CMA) for doing Auger
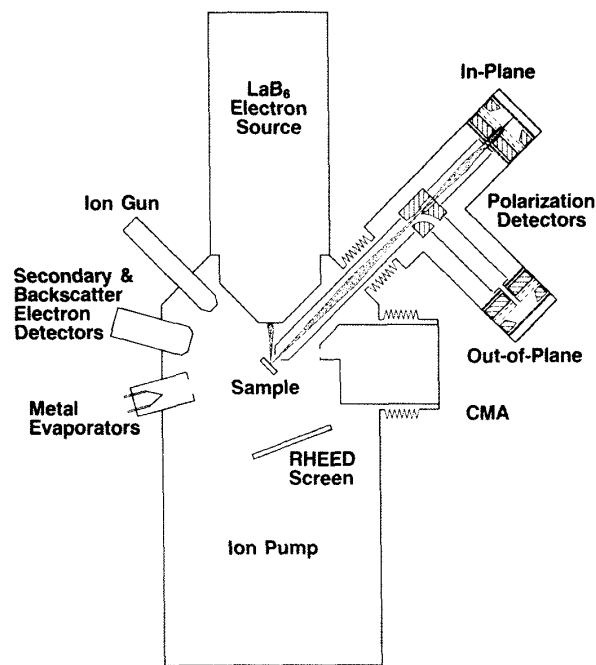
Figure 1: SEMPA apparatus schematic.

spectroscopy, an ion gun for cleaning and depth profiling samples, metal evaporators and a Reflection High Energy Diffraction (RHEED) screen for monitoring film structure during evaporation. The samples were cleaned by sputtering with 1 keV Argon ions. Surface cleanliness and chemical composition were monitored by Auger analysis. The permalloy elements were about 40 nm thick and were deposited upon a silicon substrate.

RESULTS

Figure 2 shows an example of single SEMPA measurement of a typical permalloy element. The intensity, I, and the two in-plane magnetization components, M_x and M_y, were simultaneously measured using one detector. Also shown are the magnitude of the in-plane magnetization, M, and the angle, θ, which were calculated from

$$M = \sqrt{M_x^2 + M_y^2} \ , \quad \theta = tan^{-1}(M_x/M_y) \qquad (3)$$

In this case the instrumental asymmetry was determined by assuming that both the instrumental asymmetry and the total magnetization were constant throughout the image. There still appears to be some missing magnetization at the domain walls. This is an instrumental effect, however, caused by the incident electron beam averaging over domain walls where a magnetization component changes sign in a region smaller than the beam diameter. The beam diameter for these images was about 100 nm. Since the amount of missing magnetization is directly related to the sharpness of the wall, this image shows that the domain walls that make up the arms of the y-domain are thinner than the wall that forms the leg. There is also the indication of a sharp singularity at the junction of the walls. No perpendicular magnetic component was observed for any of the elements either within the domains or at the domain walls. A problem with the method of instrumental asymmetry removal used in this image is that the absolute values of the total magnetization cannot be determined.

Note how the background nonmagnetic Si substrate appears to have the same magnetization as the permalloy.
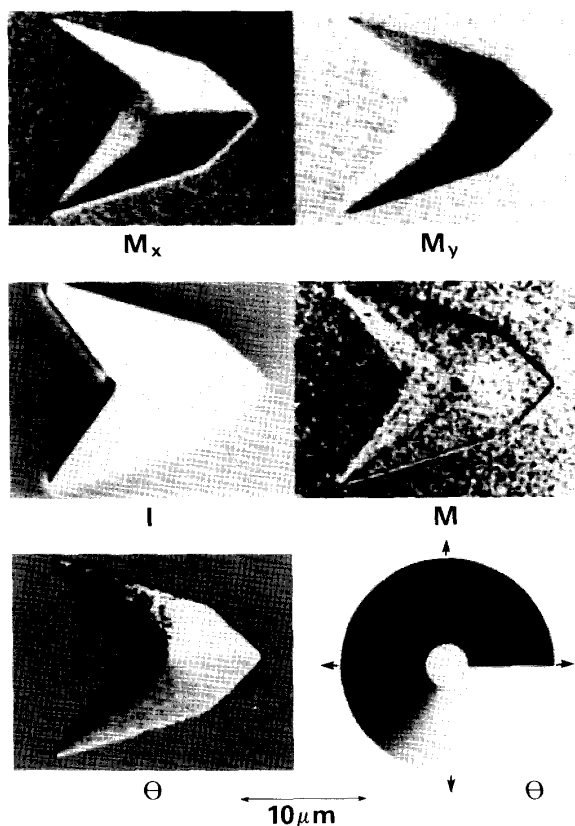

Figure 2: SEMPA image of memory element showing in-plane horizontal (M_x) and vertical (M_y) magnetization components, intensity (I), total magnetization magnitude (M) and direction (θ). The gray map key for the θ image is shown.
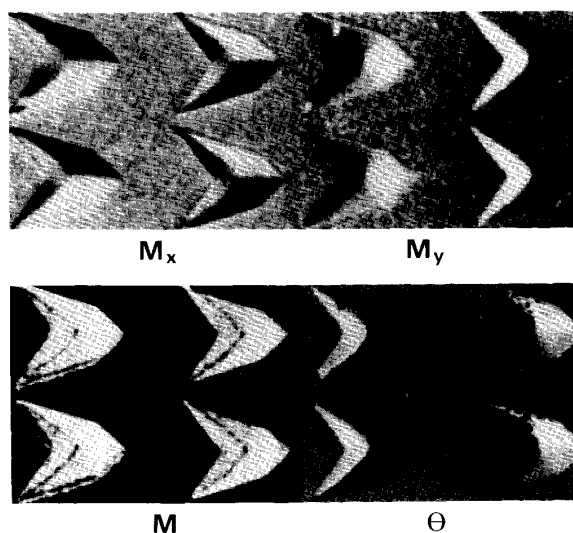

Figure 3: Same measurements as in Fig. 2, but the graphite measured instrumental asymmetry has been removed.

Figure 3 is an example of a SEMPA measurement in which the instrumental asymmetries were determined by using the detector with a spin-independent target as a reference. Four memory elements are imaged with the magnetization of the two elements on the right going around the element in a clockwise sense as opposed to counter-clockwise for the two on the left. Polarizations were first measured using the usual gold film target. The images were then repeated using a graphite target. The difference between the gold and graphite measurements are shown as M_x and M_y, as well as the calculated magnitude and angle of in-plane magnetization. In this case, not only is the magnetization uniform over the entire element, but the value is also significant. The non-magnetic substrate polarization is zero while the permalloy polarization is about 13%. The main problems associated with this method are that the signal-to-noise is decreased by $\sqrt{2}$ and, if the two images are 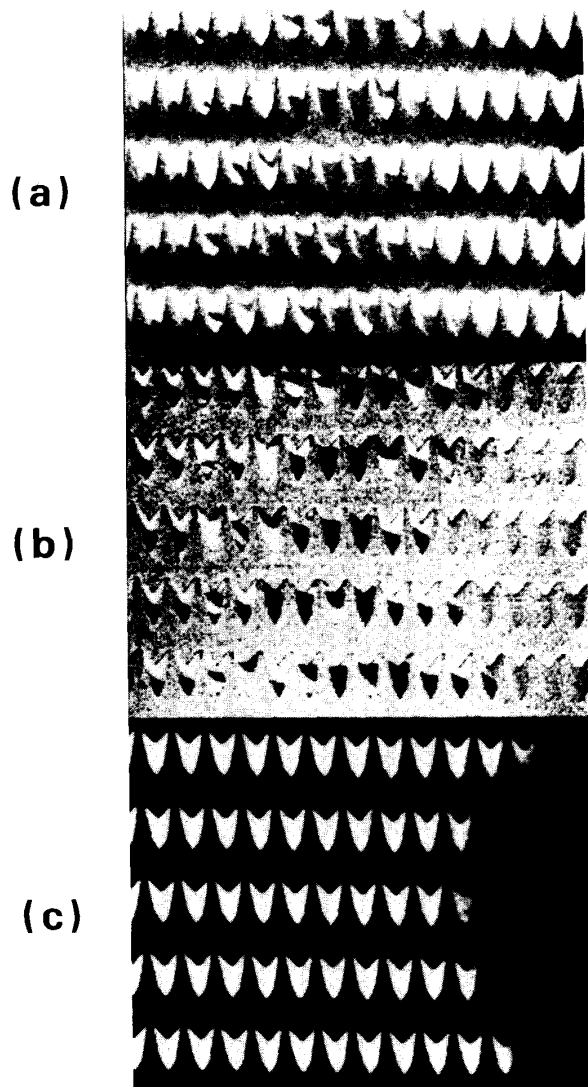not exactly aligned before subtraction, the to-pographic polarization contrast from sharp edges increases rather than decreases.

Figure 4 is an example of how SEMPA can be used as an in situ magnetic imaging technique during thin film preparation. In this case, the film is being ion milled using a stationary ion beam off to the side of the image. From the Ni Auger map (c) one can see that the permalloy has been removed from the right hand side of the image and is still intact on the left hand side. The thickness of the thinned elements in the middle of the picture is unknown, since the Auger electron depth sensitivity is only about 5 nm. One component of the in plane magnetization, M_x, is shown both with (b) and without (a) the graphite target image subtracted. As the material is removed the domains are observed to change from the standard y-domain configuration to a two domain pattern which bisects the element across its width. Note that in the graphite corrected data the polarization of the elements with no permalloy present is zero, in contrast to the uncorrected data where some instrumental polarization is observed.

CONCLUSION

Two methods of determining and eliminating spurious apparatus asymmetries in SEMPA measurements were successfully used to image the vector magnetization in permalloy memory elements. The first relied on assumptions about the symmetry of the domain pattern to establish the polarization zero. In general, this produced accurate maps of the magnetization direction as long as false asymmetries due to surface topography were not important. The second method used the spin-independent scattering from a graphite target as a reference. This method eliminated the instrumental and topographic asymmetry, and is preferred for absolute, quantitative magnetization measurements. Both methods permit one to measure the angle of the magnetization vector to within ± 10 deg.

(a)

(b)

(c)

Figure 4: Ion milled memory elements. M_x is shown before (a) and after (b) instrumental asymmetry correction. (c) Ni Auger map.

References

[1] G.G. Hembree, J. Unguris, R.J. Celotta and D.T. Pierce, Scanning Microscopy Supplement 1, 229 (1987).

[2] K. Koike, H. Matsuyama and K. Hayakawa, Scanning Microscopy Supplement 1, 241 (1987).

[3] D.T. Pierce, R.J. Celotta, M.H. Kelley and J. Unguris, Nucl. Instrum. Methods A266, 550 (1988).

[4] M.R. Scheinfein, D.T. Pierce, J. Unguris, J.J. McClelland, R.J. Celotta and M.H. Kelley, Rev. Sci. Instrum. 60, 1 (1989).

[5] D.S. Lo, G.J. Cosimini, L.G. Zierhut, R.H. Dean and M.C. Paul, IEEE Trans. Mag., MAG-21 1776 (1985).

[6] G.J. Cosimini, D.S. Lo, L.G. Zierhut, M.C. Paul, R.H. Dean and K.J. Matysik, IEEE Trans. Magnetics 24, 2060 (1988).

[7] J. Unguris, D.T. Pierce and R.J. Celotta, Rev. Sci. Instrum. 57, 1314 (1986).